



Effects of crop residue cover and architecture on heat and water transfer at the soil surface

G.N. Flerchinger^{a,*}, T.J. Sauer^b, R.A. Aiken^c

^a*Northwest Watershed Research Center, USDA Agricultural Research Service, 800 Park Boulevard, Plaza IV, Suite 105, Boise, ID 83712, USA*

^b*National Soil Tilth Laboratory, USDA Agricultural Research Service, Ames, IA, USA*

^c*Kansas State University, Colby, KS, USA*

Abstract

Different residue types and standing stubble versus distributed flat residues affect heat and water transfer at the soil surface to varying degrees. Understanding the effects of various residue configurations can assist in better residue management decisions, but this is complex due to various interacting influences. Therefore, modeling the effects of crop residues on heat and water movement can be an effective tool to assess the benefits of differing residues types and architectures for various climates. The purpose of this study was to test the ability of the Simultaneous Heat And Water (SHAW) model for simulating the effects of residue type and architecture on heat and water transfer at the surface and to evaluate the impacts of differing residue types and architectures on heat and water transfer in significantly different climates. The model was tested on bare tilled soils and corn, wheat and millet residues having varying amounts of standing and distributed flat residues for three separate locations: Ames, IA, Akron, CO and Pullman, WA. Modifications to the model were necessary to correctly simulate the effect of wind on convective transfer through a flat corn residue layer. Model efficiencies for simulated soil temperature approached or exceeded 0.90 for nearly all residue treatments and locations. The root mean square deviation for simulated water content compared to measured values was typically around $0.04 \text{ m}^3 \text{ m}^{-3}$. Satisfied that the model could reasonably simulate the effect of residue type and architecture, the model was applied to simulate the effects of differing residue architectures to 30 years of generated weather conditions for four diverse climate stations: Boise, ID; Spokane, WA; Des Moines, IA; Minneapolis, MN. Simulated frost depths for bare and standing residues were typically deeper than for flat residues. Bare soil had the highest evaporation at all sites, and flat wheat residue generally had the lowest evaporation. The wetter climates (Des Moines and Minneapolis) tended to favor flat residues for reducing evaporation more so than the drier climates. Near-surface soil temperature under standing residues warmed to 5 °C in the spring by as much as 5–9 days earlier compared to bare and flat residue cover depending

* Corresponding author. Tel.: +1-208-422-0716; fax: +1-208-334-1502.

E-mail address: gflerchi@nwr.ars.usda.gov (G.N. Flerchinger).

on location, which can have important ramifications for early seedling germination and plant establishment.

© 2003 Elsevier Science B.V. All rights reserved.

Keywords: Evaporation; Soil freezing; Soil frost; Soil temperature; Corn residue; Wheat residue

1. Introduction

Residue and tillage management are important tools for conserving soil and water resources. The presence of residue on the soil surface significantly impacts evaporation, soil water storage, soil temperature, soil freezing and associated frozen-soil runoff, as well as infiltration, runoff and erosion. This is accomplished by altering heat and water transfer rates at the soil surface. Residue architecture, meaning standing versus distributed flat residue, influences heat and water transfer from the surface. The option to till, leave standing residue, or chop and distribute residues on the surface is a critical management decision for crop establishment and soil and water conservation.

Thermal and vapor transport properties of different residue types and architectures have had limited attention and remain poorly understood. [Bristow et al. \(1986\)](#) simulated the effects of flat wheat residue on heat and water transfer and expressed convective transfer through wheat residue as a function of wind speed within the residue. [Shen and Tanner \(1990\)](#) measured radiative and conductive heat transport properties of chopped corn residue. [van Donk and Tollner \(2000a,b\)](#) studied free and forced convective heat transfer mechanisms for flat wheat straw, pine straw and bare soil. [Sauer et al. \(1996, 1997, 1998\)](#) studied the surface energy balance, temporal changes in the radiation balance and aerodynamic characteristics of standing corn stubble. [Aiken et al. \(1997\)](#) collected temperature and water measurements beneath corn, millet, sunflower and wheat residues with various architectures. [Sharratt et al. \(1998\)](#) and [Sharratt \(2002a,b\)](#) examined the effects of corn residue architecture and stubble height on soil frost, thaw and springtime temperatures.

Limited studies on residue type and architecture coupled with the complex interactions of different types of residue and architectures with different climatic conditions make it difficult to discern the benefits and disadvantages of residue management options. Different residue types and architectures affect heat and water transfer in significantly different ways, and the effects of crop residue can depend on climatic conditions. Thus, modeling the effects of crop residues on heat and water movement can be an effective tool to assess the benefits of differing residue types and architectures for various climates.

The Simultaneous Heat And Water (SHAW) model is a one-dimensional model originally developed to simulate soil freezing and thawing ([Flerchinger and Saxton, 1989a](#)). The ability of the model to simulate heat and water movement through plant cover, snow, residue and soil for predicting climate and management effects on soil freezing, snowmelt, soil temperature, soil water, evaporation and transpiration has been demonstrated ([Flerchinger and Hanson, 1989](#); [Flerchinger and Pierson, 1991](#); [Xu et al., 1991](#); [Flerchinger et al., 1994, 1996a,b, 1998](#); [Hayhoe, 1994](#); [Flerchinger and Seyfried, 1997](#),

Kennedy and Sharratt, 1998; Duffin, 1999; Hymer et al., 2000). However, the model has had limited application to varying types of residues and architectures.

The objectives of this paper are (a) to test the ability of the SHAW model for simulating the effects of crop residue on heat and water transfer and (b) to evaluate the impacts of differing residue types and architectures on heat and water transfer in significantly different climates. Simulations of the surface energy balance, evaporation, soil freezing, soil temperature and soil water content by the SHAW model were evaluated at three different locations having varying residue types and architectures. The model was then applied to a 30-year weather record to assess the advantages of different residue types and architectures for diverse climates.

2. Field sites

Data were collected for various tillage and residue treatments during the winter of 1994–1995 near Ames, IA, throughout the 1986–1987 fallow season near Pullman, WA and during 1995–1996 near Akron, CO. Model simulations were compared with (a) surface energy balance measurements over standing corn residue for Ames, IA, (b) soil temperature and water content measurements for different residue types and architectures from Akron, CO and (c) soil frost, temperature and water content measurements for flat wheat residue near Pullman, WA. A summary of residue cover characteristics for the sites is given in Table 1.

2.1. Ames site

Data collected at the Ames site are described by Sauer et al. (1998), where energy balance data and soil temperature profiles were collected for a harvested, no-till corn field. Average stalk height was 0.3 m, with over 60,000 standing stalks per hectare.

Table 1
Residue properties for the simulated field conditions

Site/treatment	Flat residue loading (kg/ha)	Residue cover (%)	Thickness of flat residue layer (cm)	Standing stem area index ($\text{m}^2 \text{m}^{-2}$)	Stem height (cm)
Ames, IA					
Standing corn stubble	8700	95	5.0	0.30	30
Akron, CO					
Bare soil	0 ^a	0	0	0.01 ^b	5
Standing corn stubble	2900	39	1.0	0.03 ^b	0.38
Flat millet residue	2500 ^a	57	1.0	0.05 ^b	11
Standing wheat stubble	5600 ^a	85	2.5	0.31	23
Pullman, WA					
Bare soil (tilled wheat)	0	0	0	0.0	0.0
Flat wheat residue	10,415	91	3.0	0.0	0.0

^a Estimated values.

^b Standing stubble assumed negligible and not included in simulation.

Estimated stem area index of standing stalks was 0.30. A significant layer of flat residue consisting of leaves, stalk fragments and cobs covered approximately 95% the soil surface.

The study site was in a 45-ha field on a Canisteo silty clay loam (fine–loamy, mixed [calcareous], mesic Typic Haplaquoll). Meteorological sensors collected 30-min weather observations of air temperature, wind speed, humidity and solar radiation. Precipitation measurements were obtained from a National Weather Service Station approximately 10 km from the field site. Soil temperatures were collected at depths of 1, 5, 10, 25, 50 and 90 cm. Energy balance was measured using a Bowen ratio energy balance system; specifics of the energy balance measurements are described in [Sauer et al. \(1998\)](#). Net radiation and soil heat flux (corrected for heat storage above the heat flux plates using periodic measurements of surface soil moisture and bulk density) were monitored continuously, while measurements for sensible and latent heat flux were limited to the fall and spring seasons and short periods during the winter.

2.2. Akron site

Data collected at the Akron site are described by [Aiken et al. \(1997\)](#), where soil temperature and moisture measurements were collected during the 1995–1996 winter for stubble mulched wheat (bare soil), no-till standing wheat stubble, no-till millet residue, no-till standing corn residue and sunflower residue. Stubble mulch wheat, no-till millet, no-till wheat and no-till corn represented a broad range of residue types and architectures and were therefore selected for model application. The sunflower plot had very little remaining residue and was not used in this analysis.

The study site was located on a Weld silt loam (fine montmorillonitic, mesic Aridic Paleustoll) soil. Hourly weather measurements included air temperature, wind speed, humidity and solar radiation; hourly soil temperatures were measured near the surface and at depths of 3, 7, 15 and 25 cm. Soil water potential observations corrected for temperature were estimated from gypsum soil moisture blocks installed at depths of 3, 7, 15 and 25 cm. Additionally, soil water content was measured periodically with vertically installed 30-cm TDR rods and with a neutron probe at depths of 45, 75, 105, 135 and 165 cm. Break-point precipitation observations were collected from a shielded, weighing precipitation gauge. Surface residue cover and standing stems (height, frequency and diameter) were quantified using a 100-point line intercept method. Standing stem observations were used to estimate the stem area index.

2.3. Pullman site

Data collected for the 1986–1987 winter at the Pullman site are described by [Flerchinger and Saxton \(1989b\)](#), who used it as the original test of the SHAW model. Data were collected for six tillage-residue conditions for winter wheat. The extremes in plot conditions were a heavy residue no-till plot and a light residue cover tilled with a rotary hoe to represent a conventionally tilled plot. [Flerchinger and Saxton \(1989b\)](#)

examined only the winter period; in the current study, data were simulated through the summer period as well.

The site was located on a south-facing Palouse silt loam (fine–silty mixed mesic Pacific Ultic Haploxeroll) soil on the USDA Palouse Conservation Field Station. Measured atmospheric data for the site included hourly air temperature, wind speed, humidity, solar radiation and precipitation. Manual measurements of snow depth were taken throughout the winter season. Soil temperatures were measured near the surface and at depths of 7.5, 15, 25, 38, 53, 69, 84, 107, 137 and 168 cm. Soil frost depth was estimated from soil gypsum blocks read every 3 h. Soil water content measurements were collected approximately weekly using a combination of gravimetric samples for depths less than 25 cm and neutron probe readings for deeper depths. Residue amount on the surface was determined from residue samples collected from 25 × 25-cm random samples.

3. Model description

The SHAW model was originally developed by Flerchinger and Saxton (1989a) and modified by Flerchinger and Pierson (1991) to include transpiring plants and a plant canopy. The physical system described by the SHAW model as presented by Flerchinger and Pierson (1991) consists of a vertical, one-dimensional profile extending from the vegetation canopy, snow, residue or soil surface to a specified depth within the soil. The system is represented by integrating detailed physics of a plant canopy, snow, residue and soil into one simultaneous solution. Interrelated heat, water and solute fluxes are computed throughout the system and include the effects of soil freezing and thawing. Daily or hourly predictions include evaporation, soil frost depth, snow depth, runoff and soil profiles of temperature, water, ice and solutes. Hourly time steps were used in this study.

The surface energy balance in the SHAW model includes solar and long-wave radiation exchange, sensible and latent heat transfer at the surface and vapor transfer within the standing residue, canopy, snow and residue. Absorbed solar radiation, corrected for local slope, is based on measured incoming short-wave radiation and includes reflection and backscattering within the canopy and residue layers. Long-wave radiation emitted by the atmosphere is estimated from the Stefan–Boltzman law and adjusted for cloud cover (estimated from measured solar radiation). Surface sensible and latent heat transfer is estimated using a bulk aerodynamic approach with stability corrections.

Detailed descriptions of energy and mass transfer calculations within the canopy, snow and residue layers are given by Flerchinger and Pierson (1991), Flerchinger et al. (1994, 1996b) and Flerchinger and Saxton (1989a), respectively. Convective heat and water transfer within standing stubble are computed much the same as within a transpiring canopy, except that the source for vapor transfer from the stubble elements is a function of water content. Heat is transferred through the residue layer by conduction through the residue elements and convection through the air voids. Evaporation and convective vapor transfer through the residue layer are described by Flerchinger and Saxton (1989a).

4. Model evaluation

Simulated and measured values were compared using the model efficiency (ME), mean bias error (MBE) and root mean square deviation (RMSD). While the latter two are self explanatory, model efficiency ($ME \leq 1$) is defined as the fraction of variation in observed values explained by the model (Nash and Sutcliffe, 1970). Definitions of model performance measures are given in Table 2.

4.1. Ames site

The model was initialized for the Ames site on day 308 (November 4), and temperature and water conditions were simulated through day 111 (April 20) for the standing corn residue field. The initial soil water content profile was obtained from a similar site within a couple of hundred meters away. Based on their similar position on the landscape, the heavy residue cover, low evaporation rates and generally wet conditions, soil water content would have been very similar at these two locations within the field.

Fig. 1 presents a comparison of measured and simulated hourly values of net radiation, sensible heat flux and latent heat flux for the first 2 weeks in April. Measured values represent hourly averages of 30-s readings. Net radiation and sensible heat flux were simulated quite well. Problems with the Bowen ratio unit are noted with the spikes in measured sensible and latent heat flux. In particular, the Bowen ratio unit had measurement problems during four cloudy days (day 99–102). On days 100 and 101 when humidity exceeded 90%, midday potential latent heat fluxes computed using the Penman equation were around -40 W/m^2 compared to measured fluxes around -85 W/m^2 ; thus, measurements during this period are likely in error. Even so, the model underpredicted the magnitude of the latent heat flux for the entire simulation period, as illustrated for the 2-week period in Fig. 1.

The consistent underprediction of latent heat flux was rather unsettling. The site had a significant layer of flat residue (Table 1), so among other things, we reassessed how the

Table 2
Description and definition of model performance measures

Measure	Description	Mathematical definition [†]
ME	model efficiency, i.e., variation in measured values accounted for by the model	$1 - \frac{\sum_{i=1}^N (Y_i - \hat{Y}_i)^2}{\sum_{i=1}^N (Y_i - \bar{Y})^2}$
RMSD	root mean square difference between simulated and observed values	$\left[\frac{1}{N} \sum_{i=1}^N (\hat{Y}_i - Y_i)^2 \right]^{1/2}$
MBE	mean bias error of model predictions compared to observed values	$\frac{1}{N} \sum_{i=1}^N (\hat{Y}_i - Y_i)$

[†] \hat{Y}_i = simulated values; Y_i = observed values; \bar{Y} = mean of observed values; N = number of observations.

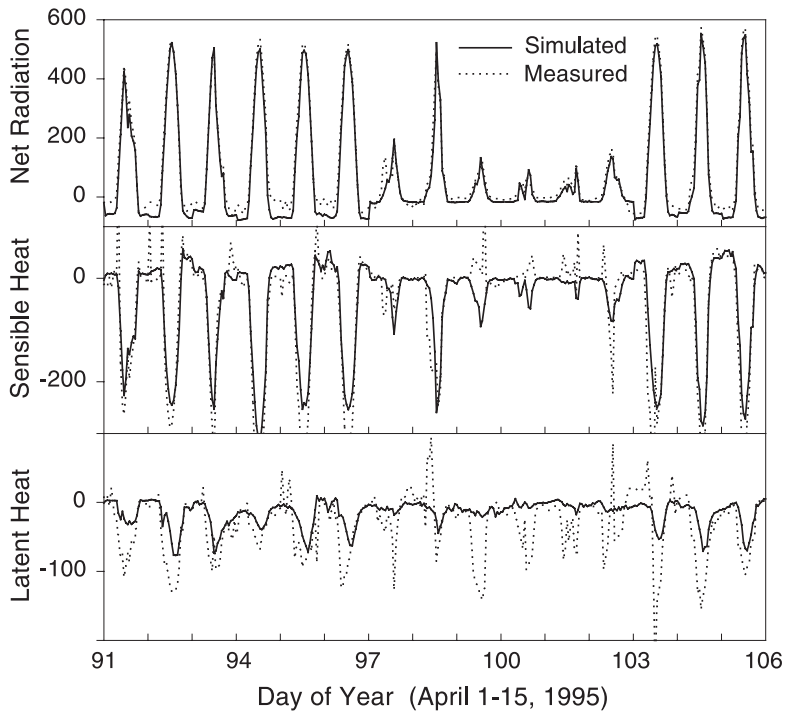


Fig. 1. Measured and simulated components of the surface energy balance over standing corn residue near Ames, IA for the first 2 weeks of April (all fluxes are in W/m^2 and assumed positive toward the surface).

model simulates convective transfer through the flat residue layer. The SHAW model uses an equation presented by [Bristow et al. \(1986\)](#) for convective transfer through wheat residues, expressed as

$$k_v = k_a(1 + 0.007T)(1 + 4u_r) \quad (1)$$

where diffusivity through the residue k_v ($\text{m}^2 \text{s}^{-1}$) is a function of diffusivity of still air k_a ($\text{m}^2 \text{s}^{-1}$) adjusted for wind speed within the residue, u_r (m/s). The term for temperature, T ($^{\circ}\text{C}$), accounts for the dependency of still air diffusivity on temperature ([Bristow et al., 1986](#)).

Previously, parameterization of Eq. (1) was assumed independent of crop residue type in the SHAW model. Realistically, the large stalks of flat corn residue create a much more open void space than does wheat residue, and wind is more effective at increasing diffusivity through the residue layer. [Tanner and Shen \(1990\)](#) presented an equation for diffusivity through an 11-mm-thick flat corn residue expressed as:

$$k_v = k_a(1 + 0.89u_{1m}) \quad (2)$$

where u_{1m} (m/s) is wind speed at 1 m above the surface. The coefficient for wind speed is 53% greater than that found by [Kimball and Lemon \(1971\)](#), 0.58, for a 20-mm wheat residue layer. [Tanner and Shen \(1990\)](#) reported 1-cm wind speeds were 38% of that at 1 m;

assuming a logarithmic wind profile above the residue layer and a linear wind speed profile within the flat residue layer, Eq. (2) becomes

$$k_v = k_a(1 + 8.5u_r) \quad (3)$$

for diffusivity at the midpoint of the residue layer, while the coefficient presented by Kimball and Lemon for wheat residue becomes 4.8 for wind speed at the midpoint of the wheat residue. Although the wind profile assumptions yield a coefficient for wheat residue similar to that of [Bristow et al. \(1986\)](#) already used in the SHAW model, the coefficient for flat corn residue is much higher.

Upon introducing the coefficient for wind speed in Eq. (3) into the model, much higher latent heat fluxes were simulated, as shown in [Fig. 2](#). The new results show a better agreement with measured results: overpredicting the magnitude in places, but still slightly underpredicting in many others. The few cloudy days with measurement difficulties are still apparent, but overall, simulation results for latent heat flux were improved significantly.

The improvement in simulation results using the appropriate coefficient for corn residue extends to soil temperatures as well. The mean bias error for the 1- and 5-cm simulated soil temperature for the entire simulation period was +0.4 and +0.1 °C using the original relationship; mean bias error decreased to +0.3 and 0.0 °C using the appropriate coefficient for corn residue. Previously, the limited thermal diffusivity through the residue limited evaporation from the soil surface and resulted in simulated soil temperatures being too warm. Model efficiency increased from 0.80 and 0.86 to 0.82 and 0.88, respectively ([Table 3](#)).

4.2. Akron site

No-till standing wheat residue, tilled wheat residue, no-till corn residue and no-till millet residue plots were simulated for the Akron site. The model was initialized using soil moisture profiles measured on day 331 of 1995 (November 27) and estimated soil

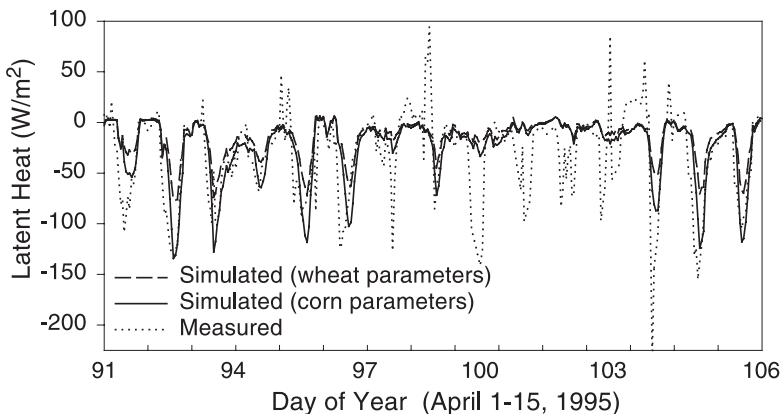


Fig. 2. Effects of using convection parameters for wheat versus corn on simulated latent heat flux over corn residue near Ames, IA (heat flux is assumed positive toward the surface).

Table 3

Comparison of simulated soil temperatures to measured soil temperatures at the Ames, Pullman and Akron sites

Site/treatment	Simulation period	Depth (cm)	ME ^a	MBE ^b (°C)	RMSD ^c (°C)
Ames, IA					
Standing corn residue	November 4–April 20	1	0.82	+0.27	1.52
		5	0.88	+0.04	1.16
Pullman, WA					
Bare soil	November 4–September 2	surface	0.89	–0.57	3.96
		7	0.95	–1.27	2.15
		15	0.96	–1.30	1.90
		25	0.96	–1.24	1.85
Flat wheat residue	November 4–September 2	surface	0.94	0.84	2.35
		7	0.97	0.87	1.40
		15	0.98	0.71	1.10
		25	NA ^d	NA	NA
Akron, CO					
Standing corn residue	November 7–June 5	surface	0.91	0.17	3.72
		15	0.90	0.33	2.23
		25	0.95	0.46	1.33
Bare soil (tilled wheat)	November 7–September 10	surface	0.96	0.30	3.06
		15	0.94	0.39	2.58
		25	0.97	0.34	1.67
Millet (no-till)	November 7–April 30	surface	0.85	–0.25	3.90
		15	0.88	0.04	1.74
		25	0.93	–0.04	1.12
Standing wheat residue	November 7–September 10	surface	0.92	0.48	3.70
		15	0.93	1.24	2.66
		25	0.96	1.03	1.84

^a ME—model efficiency.^b MBE—mean bias error.^c RMSD—root mean square deviation.^d NA—measured soil temperatures were not available due to sensor malfunction.

temperatures below the measured 25-cm profile. Values were simulated through day 156 of 1996 (June 4) for the corn and millet plots at which time measurements were discontinued. Measurements were available through day 254 (September 10) for the two wheat plots, and simulations were continued throughout the entire period; however, TDR measurements for the tilled wheat residue after day 204 (July 22) were unreliable.

Although there was much less corn residue at the Akron site compared to the Ames site, modifications to the model discussed for the Ames site also improved simulation results for the Akron no-till corn site, which had a modest amount of flat corn residue (Table 1). Fig. 3 presents simulated and measured soil surface temperatures for corn residue for the last 2 weeks in February. For illustration, simulation results using the original equation based on wheat residue are plotted along with results from the modification for corn residue. Clearly the results using the equation for corn residue compare much better with the measurements, particularly for the midday soil temperatures. Model efficiency for simulated surface soil temperature over the entire simulation

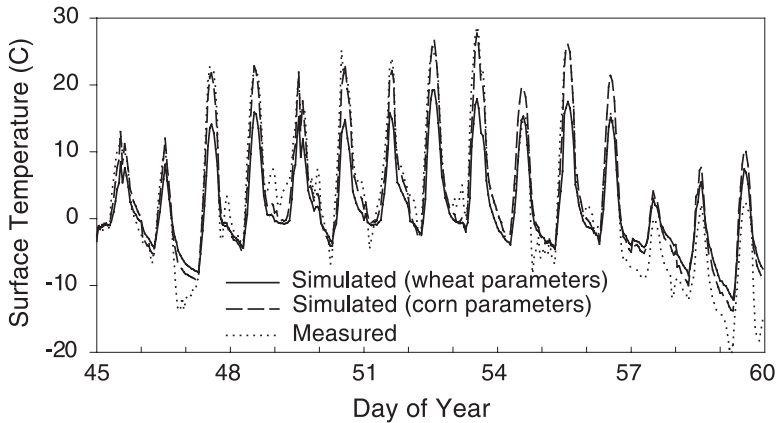


Fig. 3. Simulated and measured soil surface temperatures under corn residue near Akron, CO for the last 2 weeks in February.

period (day 326 in 1995 to day 155 in 1996) increased from 0.86 to 0.91 using the modification for corn residue.

Comparisons of simulated and measured soil temperature are given for all four residue treatments in Table 3. With the exception of the millet treatment, model efficiency exceeded 0.90 for all treatments and all depths. Model efficiency was lower for the simulated millet soil temperatures only because the simulation period was shorter and the warmer temperatures after April are absent from the analysis; this resulted in less variation in observed temperature (model efficiency is defined as the fraction of variation in observed values explained by the model; with less variation in observed values, identical absolute errors result in lower model efficiency). Indeed, simulation results for millet based on mean bias error (MBE) and root mean square deviation (RMSD) are similar or better than the other residue treatments.

Simulated total and liquid water content and TDR-measured liquid water content are plotted for the standing wheat stubble field in Fig. 4a. Simulated liquid water content agrees well with the measurements, particularly during the period of soil freezing. Simulated total water content was quite dynamic as a result of moisture migration in response to soil freezing. In contrast, results for the bare tilled field, which was much drier, are plotted in Fig. 4b. Drier conditions in the bare field resulted in much less ice formation and less water migration in response to soil freezing. The RMSD for simulated liquid water content of the top 30 cm was highest for the bare tilled soil at $0.06 \text{ m}^3 \text{ m}^{-3}$; RMSD was $0.04\text{--}0.05 \text{ m}^3 \text{ m}^{-3}$ for the other three treatments.

4.3. Pullman site

The model was parameterized for identical residue conditions as simulated by Flerchinger and Saxton (1989b). The SHAW model was initialized with soil temperature and water content profiles measured on day 308 of 1986 (November 4), and values were simulated through day 245 of 1987 (September 2). Flerchinger and Saxton (1989b)

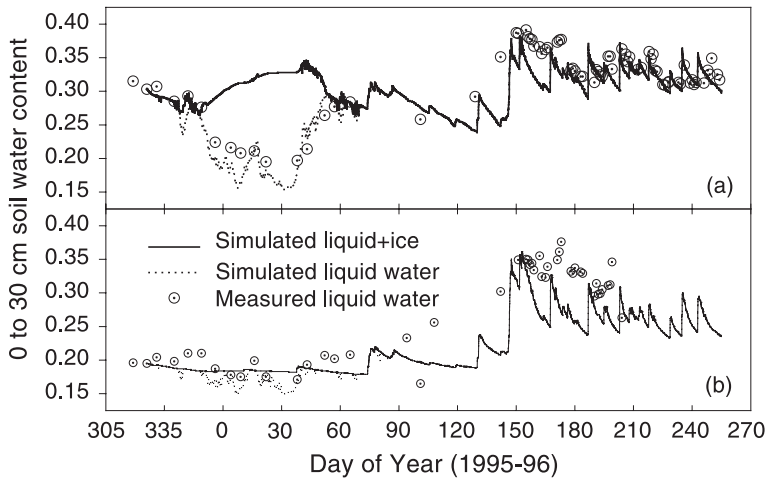


Fig. 4. Simulated total and liquid volumetric water content and TDR-measured liquid water content for (a) a standing wheat stubble field and (b) a bare tilled field near Akron, CO.

presented simulation results for snow depth and soil freezing, showing good agreement between measured and simulated values. The insulating effect of the thick residue layer for the no-till treatment limited frost depth to less than 5 cm, while the bare soil treatment had frost depth exceeding 10 cm.

Simulated and measured water content is plotted for the bare soil site in Fig. 5. The 7-cm water content was simulated quite well; however, the 15-cm water content was overpredicted by approximately $0.08 \text{ m}^3 \text{ m}^{-3}$. This is likely due to the fact that the

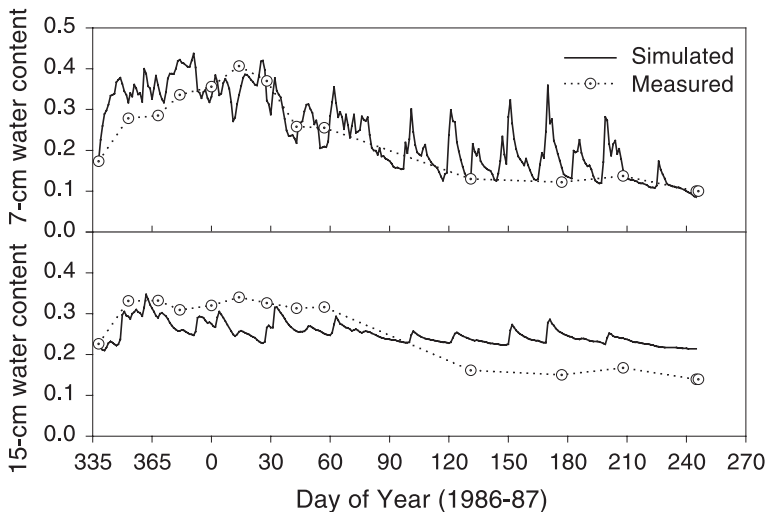


Fig. 5. Simulate and measured volumetric water content for a bare tilled soil near Pullman, WA.

model does not account for additional opportunity for evaporation from cracked soils, which was prevalent for this plot. The RMSD for the simulated surface, 7, 15 and 25 cm water contents were 0.07, 0.08, 0.06 and 0.04 $\text{m}^3 \text{m}^{-3}$ for the bare tilled site and 0.05, 0.09, 0.04 and 0.05 for the no-till flat wheat residue. Comparison of simulated and measured soil temperatures are given in Table 3.

5. Simulated effects

Measurements presented in the previous section give clues into the effects of residue cover and architecture on heat and water transfer at the surface, but differing initial soil water conditions, residue loadings and locations make it difficult to make direct comparisons between differing residue types and architectures for different climatic conditions. However, simulation results from the preceding section do suggest that the model can reasonably simulate residue cover effects on heat and water transfer and the resulting influence on soil frost, temperature, evaporation and soil water. Satisfied that the model performs reasonable well, we used the model to simulate the effects of differing residues and architectures for various climates.

For this analysis, 35 years of weather were generated for four locations using the GEM model, a stochastic weather generator (Hanson and Johnson, 1998). This model stochastically generates daily values of maximum and minimum temperature, wind speed, solar radiation, dew point and precipitation which maintain the statistical relevance for a given location. Sites were selected based on availability of GEM model parameters sets, proximity to measurement sites and climate diversity. Sites included Boise, ID, Spokane, WA, Des Moines, IA and Minneapolis, MN. A climate summary for each location is given in Table 4. Daily values generated by the GEM model were disaggregated to hourly values by routines within the SHAW model.

The first 5 years of generated weather were used to allow the simulated soil temperatures to equilibrate to climatic conditions. Thirty 1-year simulations were then conducted for each treatment at each location by resetting the soil water profile at the beginning of each yearly simulation. The soil water profile was reset on October 1 of each year to a

Table 4
Climate summary for 30-year generated weather sequence

	Boise	Spokane	Des Moines	Minneapolis
Latitude	43°34'	47°37'	41°31'	44°52'
Longitude	116°13'	117°31'	93°39'	93°13'
Elevation (m)	874	721	294	255
Precipitation (mm)	306	405	760	704
Normal maximum annual temperature (°C)	42	38	39	38
Normal minimum annual temperature (°C)	– 17	– 18	– 26	– 30
Average maximum annual snow depth (simulated, cm)	19	31	25	35
Average wind (m/s)	7.5	8.2	9.4	9.3

uniform water content of -50 bars ($0.150 \text{ m}^3 \text{ m}^{-3}$) and the model was run through the following September 30.

To eliminate the effect of soil type and to better isolate residue effects between locations, soil parameters were assumed identical for all locations. A typical silt loam soil was assumed; actual soils found at these locations range from silt loam to silty clay loam. Subsequent simulations indicated that the slight change in soil texture did influence the magnitude of values used for comparisons, but relative differences between residue conditions remained relatively unchanged.

Five residue conditions were examined: bare soil; standing wheat stubble; flat wheat residue; standing corn stubble; flat corn residue. For the residue simulations, a typical post-harvest residue loading of 6000 kg/ha of wheat or 10,000 kg/ha of corn was assumed. This was distributed between standing and flat residue for the standing stubble simulations. Assumed configurations for the five residue conditions are given in Table 5. Effects of residue condition on frost depth, evaporation and springtime soil warming were examined.

5.1. Frost depth

Effects of residue on simulated frost depth are summarized in Table 6. In general, the bare site had the deepest average annual frost depth for each location; however, this was not always significantly different from the residue-covered sites. Flat corn residue generally had the shallowest frost depth for all sites. Frost depth was less for flat wheat residue than for the two standing residue treatments, but not significantly for all sites. Frost depth for standing residue tended to vary more from year to year compared to the other conditions, indicating that these sites are more sensitive to year-to-year variation in weather conditions.

Simulated expected frost for Minneapolis ranged from around 30 to 115 cm, depending on residue cover, with an average of around 75 cm. These numbers agree with observations made by Sharratt et al. (1998) who reported frost depths between 40 and 110 cm for a 3-year study near Morris, MN. Longer term observations closer to Minneapolis show frost depths ranging from 30 to 100 cm (Baker, 2001, personal communication).

Table 5
Assumed residue properties for thirty 1-year simulations

Treatment	Flat residue loading (kg/ha)	Residue cover (%)	Thickness of flat residue layer (cm)	Standing stem area index ($\text{m}^2 \text{ m}^{-2}$)	Stem height (cm)
Bare soil	0	0	0	0.0	0
Standing wheat	1500	30	0.3	0.31	23
Flat wheat residue	6000	95	2.5	0.0	0
Standing corn	2500	30	1.0	0.30	30
Flat corn residue	10,000	95	5.0	0.0	0

Table 6

Thirty-year average simulated annual frost depth (and standard deviation) in centimeters for various residue conditions

Treatment	Boise, ID	Spokane, WA	Des Moines, IA	Minneapolis, MN
Bare soil	26.4 ab (7.3)	35.6 a (11.2)	54.4 ab (11.9)	85.7 a (17.6)
Standing wheat	26.8 a (8.1)	32.3 ab (11.0)	52.9 a (14.4)	78.5 b (21.5)
Flat wheat residue	22.5 c (7.4)	28.6 c (11.6)	50.0 c (11.7)	79.8 b (17.9)
Standing corn	26.3 b (7.9)	31.0 bc (10.4)	52.1 bc (14.0)	70.4 c (21.1)
Flat corn residue	19.0 d (5.8)	25.3 d (10.4)	45.7 d (13.4)	66.8 c (16.0)

Values followed by the same letter in the same column are not significantly different at $p=0.05$ confidence level based on a paired Student's *t*-test.

5.2. Evaporation

Effects of residue on evaporation are summarized in Table 7. Regardless of location, the bare soil consistently had the highest evaporation, while the flat wheat residue usually had the lowest evaporation. Residue architecture effects were more pronounced in Des Moines and Minneapolis compared to Boise and Spokane. The range in average evaporation between different residue architectures is 13 and 16 mm for the Spokane and Boise sites, which is less than 8% of the annual evaporation, while the range for the Des Moines and Minneapolis sites are 80 and 66 mm, or around 20% of the annual evaporation. The increased effect of architecture for the mid-west locations is likely due to the flat residue effectively preserving summertime precipitation, particularly for Des Moines. Summers are very dry in the Spokane and Boise, and residue architecture made little difference in preserving moisture from the relatively small rainfall events. Larger summertime precipitation events in the mid-west were able to penetrate through the residue and deeper into the soil, enabling the residue cover to preserve a larger portion of the rain water.

5.3. Spring warming

We used the last day of the winter/spring season on which the 5-cm soil temperature was less than 5 °C as an indication of springtime soil warming. Although this might be somewhat arbitrary, it is illustrative nonetheless. Standing residue consistently warmed faster at all sites than other residue conditions (Table 8). With more soil exposed, surfaces

Table 7

Thirty-year average simulated annual evaporation (mm) for various residue conditions

Treatment	Boise, ID	Spokane, WA	Des Moines, IA	Minneapolis, MN
Bare soil	260 a	271 a	578 a	518 a
Standing wheat	209 d	206 d	446 d	393 c
Flat wheat residue	213 c	204 d	376 e	333 e
Standing corn	213 c	209 c	456 b	399 b
Flat corn residue	225 b	217 b	421 c	372 d

Values followed by the same letter in the same column are not significantly different at $p=0.05$ confidence level based on a paired Student's *t*-test.

Table 8

Average last day of the year during the late winter/early spring season with simulated 5-cm soil temperature colder than 5 °C for various residue conditions

Treatment	Boise, ID	Spokane, WA	Des Moines, IA	Minneapolis, MN
Bare soil	87 a	102 a	100 a	110 ab
Standing wheat	82 b	93 b	93 b	103 d
Flat wheat residue	89 a	100 a	99 a	109 b
Standing corn	83 b	95 b	93 c	104 c
Flat corn residue	90 a	102 a	99 a	110 a

Values followed by the same letter in the same column are not significantly different at $p=0.05$ confidence level based on a paired Student's *t*-test.

with standing residues have a lower albedo, absorb more solar radiation than flat residues and are more efficient at trapping and retaining the heat than the bare soil. As a result, standing residues warmed 5–9 days earlier than other treatments depending on the location. Earlier soil warming under standing residue has been observed by Sharratt et al. (1998).

6. Summary and conclusions

The Simultaneous Heat And Water (SHAW) model was used to simulate the effects of differing crop residues and architectures on heat and water transfer at the soil surface for three field sites. The model was applied to standing corn residue near Ames, IA; standing wheat stubble, flat corn and millet residue and a bare tilled field near Akron, CO; flat wheat residue and bare tilled field near Pullman, WA. Previously, the model has had limited application to varying types of residues and architectures.

It was shown that the assumptions in the model regarding convective heat transfer through residue were inadequate to simulate heat and vapor transfer through flat corn residue. Model modifications were made for appropriate parameterization of the model for the effect of wind on convective transfer through corn residue. Simulations of latent heat flux and soil temperature for a relatively heavy corn residue at the Ames field location were improved after model modifications. The same modification was also shown to improve simulated soil temperature for a relatively sparse corn residue layer at the Akron site.

Model efficiency for simulated soil temperature exceeded 0.90 for most field treatments and locations. Root mean square deviation (RMSD) ranged from 3.0 to 4.0 °C for surface temperatures, and decreased to between 1.1 and 1.9 °C for 25-cm soil temperatures. RMSD for simulated soil water content was typically around $0.04 \text{ m}^3 \text{ m}^{-3}$, but ranged as high as $0.09 \text{ m}^3 \text{ m}^{-3}$ for a cracked bare soil; provisions for the effect on soil cracking on enhanced vapor transport is not considered in the model.

Simulation results suggest that the model can reasonably simulate residue cover effects on heat and water transfer and the resulting influence on soil frost, temperature, evaporation and soil water. Satisfied that the model performs reasonably well, we used the model to simulate the effects of differing residues and architectures for various

climates. The model was applied to 30-year generated weather records to assess the advantages of different residue types and architectures for four diverse climates: Boise, ID; Spokane, WA; Des Moines, IA; Minneapolis, MN.

Simulated frost depths for bare and standing residues were deeper than flat residues, although not always significantly so. Varying weather conditions from year to year even at a given location could alter the surface energy balance sufficiently to enhance or suppress heat and water exchange differently from the different residue architectures. The complicating effects of snow capture by standing residue were not considered and may be a factor in some locations, as observed by Sharratt et al. (1998).

Bare soil had the highest evaporation at all sites, and flat wheat residue generally had the lowest evaporation. The wetter climates tended to favor flat residues for reducing evaporation more than the drier climates. Standing residues warmed earlier in the spring by as much as 5–9 days compared to bare and flat residue sites depending on location, which can have important ramifications for early seedling germination and plant establishment.

References

- Aiken, R.A., Nielsen, D.C., Vigil, M.F., Ahuja, L.R., 1997. Field evaluation of energy balance simulation of surface soil temperatures. Proceedings of the International Wind Erosion Symposium, Manhattan, Kansas, June 3–5, 1997. USDA-ARS Wind Erosion Research Center, Manhattan, KS, pp. 1–12. <http://www.weru.ksu.edu/symposium/proceedings/aiken.pdf>.
- Bristow, K.L., Campbell, G.S., Papendick, R.I., Elliott, L.F., 1986. Simulation of heat and moisture transfer through a surface residue-soil system. *Agric. For. Meteorol.* 36, 193–214.
- Duffin, E.K., 1999. Evaluating snowmelt runoff, infiltration, and erosion in a sagebrush-steppe ecosystem. Master's thesis, Watershed Science Program, Utah State University, Logan, UT. 159 pp.
- Flerchinger, G.N., Hanson, C.L., 1989. Modeling soil freezing and thawing on a rangeland watershed. *Trans. Am. Soc. Agric. Eng.* 32 (5), 1551–1554.
- Flerchinger, G.N., Pierson, F.B., 1991. Modeling plant canopy effects on variability of soil temperature and water. *Agric. For. Meteorol.* 56, 227–246.
- Flerchinger, G.N., Saxton, K.E., 1989a. Simultaneous heat and water model of a freezing snow–residue–soil system: I. Theory and development. *Trans. Am. Soc. Agric. Eng.* 32 (2), 565–571.
- Flerchinger, G.N., Saxton, K.E., 1989b. Simultaneous heat and water model of a freezing snow–residue–soil system: I. Field Verification. *Trans. Am. Soc. Agric. Eng.* 32 (2), 573–578.
- Flerchinger, G.N., Seyfried, M.S., 1997. Modeling soil freezing and thawing and frozen soil runoff with the SHAW model. In: Iskandar, I.K., Wright, E.A., Radke, J.K., Sharratt, B.S., Groenevelt, P.H., Hinzman, L.D. (Eds.), Proceedings of the International Symposium on Physics, Chemistry, and Ecology of Seasonally Frozen Soils, Fairbanks, AK, June 10–12, 1997. CRREL Special Report 97-10. U.S. Army Cold Regions Research and Engineering Laboratory, Hanover, NH, pp. 537–543.
- Flerchinger, G.N., Cooley, K.R., Deng, Y., 1994. Impacts of spatially and temporally varying snowmelt on subsurface flow in a mountainous watershed: 1. Snowmelt simulation. *Hydrol. Sci. J.* 39, 507–520.
- Flerchinger, G.N., Baker, J.M., Spaans, E.J.A., 1996a. A test of the radiative energy balance of the SHAW model for snowcover. *Hydrol. Proc.* 10 (10), 1359–1367.
- Flerchinger, G.N., Hanson, C.L., Wight, J.R., 1996b. Modeling of evapotranspiration and surface energy budgets across a watershed. *Water Resour. Res.* 32 (8), 2539–2548.
- Flerchinger, G.N., Kustas, W.P., Weltz, M.A., 1998. Simulating surface energy fluxes and radiometric surface temperatures for two arid vegetation communities using the SHAW model. *J. Appl. Meteorol.* 37 (5), 449–460.
- Hanson, C.L., Johnson, G.L., 1998. GEM (Generation of weather elements for multiple applications): its appli-

- cation in areas of complex terrain. In: Kovar, K., Tappeiner, U., Peters, N.E., Craig, R.G. (Eds.), Proceedings of the HeadWater '98 Conference, Hydrology, Water Resources and Ecology in Headwaters, IASH Publ. no. 248, April, 20–23, 1998. Meran/Merano, Italy, pp. 27–32.
- Hayhoe, H.N., 1994. Field testing of simulated soil freezing and thawing by the SHAW model. *Can. Agric. Eng.* 36 (4), 279–285.
- Hymer, D.C., Moran, M.S., Keefer, T.O., 2000. Soil water evaluation using a hydrologic model and calibrated sensor network. *Soil Sci. Soc. Am. J.* 64 (1), 319–326.
- Kennedy, I., Sharratt, B., 1998. Model comparisons to simulate frost depth. *Soil Sci.* 163 (8), 636–645.
- Kimball, B.A., Lemon, E.R., 1971. Air turbulence effects upon soil gas exchange. *Soil Sci. Soc. Am. Proc.* 35, 16–21.
- Nash, J.E., Sutcliffe, J.V., 1970. River flow forecasting through conceptual models: Part I. A discussion of principles. *J. Hydrol.* 10 (3), 282–290.
- Sauer, T.J., Hatfield, J.L., Prueger, J.H., 1996. Aerodynamic characteristics of standing corn stubble. *Agron. J.* 88 (5), 733–739.
- Sauer, T.J., Hatfield, J.L., Prueger, J.H., 1997. Over-winter changes in radiant energy exchange of a corn residue-covered surface. *Agric. For. Meteorol.* 85, 279–287.
- Sauer, T.J., Hatfield, J.L., Prueger, J.H., Norman, J.M., 1998. Surface energy balance of a corn residue-covered field. *Agric. For. Meteorol.* 89, 155–168.
- Sharratt, B.S., 2002a. Corn stubble height and residue placement in the northern US Corn Belt: I. Soil physical environment during winter. *Soil Tillage Res.* 64, 243–252.
- Sharratt, B.S., 2002b. Corn stubble height and residue placement in the northern US Corn Belt: II. Spring microclimate and wheat development. *Soil Tillage Res.* 64, 253–261.
- Sharratt, B.S., Benoit, G.R., Voorhees, W.B., 1998. Winter soil microclimate altered by corn residue management in the northern Corn Belt of the USA. *Soil Tillage Res.* 49, 243–248.
- Shen, Y., Tanner, C.B., 1990. Radiative and conductive transport of heat through flail-chopped corn residue. *Soil Sci. Soc. Am. J.* 54, 653–658.
- Tanner, C.B., Shen, Y., 1990. Water vapor transport through a flail-chopped corn residue. *Soil Sci. Soc. Am. J.* 54 (4), 945–951.
- van Donk, S.J., Tollner, E.W., 2000a. Measurement and modeling of heat transfer mechanisms in mulch materials. *Trans. Am. Soc. Agric. Eng.* 43 (4), 919–925.
- van Donk, S.J., Tollner, E.W., 2000b. Apparent thermal conductivity of mulch materials exposed to forced convection. *Trans. Am. Soc. Agric. Eng.* 43 (5), 1117–1127.
- Xu, X., Nieber, J.L., Baker, J.M., Newcomb, D.E., 1991. Field testing of a model for water flow and heat transport in variably saturated, variably frozen soil. *Transportation Research Record*, vol. 1307. *Transp. Res. Board, Nat. Res. Council, Washington, DC*, pp. 300–308.